

The intermediate pressure phases of cerium studied by LDA+Gutzwiller method

Ming-Feng Tian^{1,2}, Xiaoyu Deng^{2,3}, Zhong Fang², Xi Dai²

¹*Institute of Applied Physics and Computational Mathematics,
P. O. Box 8009, Beijing 100088, China*

²*Beijing National Laboratory for Condensed Matter Physics and Institute of Physics,
Chinese Academy of Sciences, Beijing 100190, China*

³*Centre de Physique Théorique, Ecole Polytechnique,
CNRS, 91128 Palaiseau Cedex, France*

(Dated: March 7, 2022)

Abstract

The thermodynamic stable phase of cerium metal in the intermediate pressure regime (5.0–13.0 GPa) is studied in detail by the newly developed local-density approximation (LDA)+ Gutzwiller method, which can include the strong correlation effect among the $4f$ electrons in cerium metal properly. Our numerical results show that the α'' phase, which has the distorted body-centered-tetragonal structure, is the thermodynamic stable phase in the intermediate pressure regime and all the other phases including the α' phase (α -U structure), α phase (fcc structure), and bct phases are either metastable or unstable. Our results are quite consistent with the most recent experimental data.

PACS numbers: 71.27.+a, 71.10.Fd, 71.20.Be

I. INTRODUCTION

Due to the strong correlation effect, the $4f$ electrons in Lanthanide metal usually participate very weakly into the chemical bonding, which makes these materials approximately s -band metal with close-packed crystal structure. A very important exception of this qualitative understanding is the cerium metal, where the $4f$ electrons participate in chemical bonding in the α fcc phase under ambient pressure. While the α fcc phase is quite close to the instability, an isostructure phase transition happens by raising the temperature above 116 K, after which the crystal structure remains unchanged while the volume expands by 16% and the $4f$ electrons become localized.[1] Further numerical studies by implementing the first-principles methods with dynamical mean-field theory[2, 3] show that the γ phase may be stabilized by the entropy.[4]

Another mysterious phenomena in cerium is the intermediate pressure phase. At zero temperature, the cerium metal forms the face-centered-cubic (fcc) structure for pressure below 5.0 GPa and body-centered-tetragonal (bct) structure for pressure above 13.0 GPa. But the experimental results of the thermodynamic stable phase in the intermediate pressure region between 5.0 and 13.0 GPa are still quite controversial,[5–10] as will be discussed below in detail.

Ellinger and Zachariassen applied x-ray-diffraction studies on high-pressure cerium with a diamond-anvil cell,[5] and they reported that for pressure between 5.0 and 13.0 GPa, the orthorhombic α' -Ce phase with an α -uranium type of structure is the thermodynamic stable phase. They also found that the α'' phase, which is monoclinic body centered with a deformed cubic face-centered structure, is the thermodynamic metastable phase. The conclusion that α' -Ce is the thermodynamic stable phase between 5.0 and 13.0 GPa while the α'' phase is metastable has been supported by some of the follow-up experiments, i.e., Refs. [6] and [7], while another group of experiments led to the opposite conclusion, which indicated that the α'' rather than the α' phase is the thermodynamic stable phase in the intermediate pressure regime. Using diamond-anvil cell and synchrotron radiation Olsen *et al.* studied the high-pressure phase diagram of cerium up to 46.0 GPa.[8] They reported that the α'' phase is the thermodynamic stable intermediate pressure phase of Ce, and no evidence for the α' phase with α -uranium structure was found. This was the first experiment reporting the α'' phase to be the thermodynamic stable intermediate pressure phase for cerium. After

that several other groups also reported similar experimental results supporting the α'' phase to be the thermodynamic stable phase of cerium for pressure between 5.0 and 13.0 GPa.[9, 10]

The first-principles calculation is a powerful theoretical tool to predict the ground-state phases of solid. During the past two decades, many efforts have been made to reveal the thermodynamic stable phase for cerium under intermediate pressure by first-principles calculations. The early results of the linear muffin-tin orbital (LMTO) method found the α' phase to be the thermodynamic stable phase in the intermediate pressure regime between the low-pressure fcc phase and high-pressure bct phase,[11, 12] which was consistent with the early experiments. After that, Söderlind and Eriksson *et al.* applied the generalized-gradient approximation (GGA) based on the full-potential linear muffin-tin orbital (FPLMTO) method to the same problem[13] and found that α'' phase was the thermodynamic stable phase only in a small pressure interval. Ravindran *et al.* have made systematic electronic structure and total-energy studies on Ce and did not find any thermodynamic stable phase in the intermediate pressure regime between the low-pressure fcc phase to the high-pressure bct phase.[14] According to their results, both the α' and α'' phases are metastable phases with the α'' phase being lower in energy. After that, local-density approximation (LDA)- or GGA-type calculations by other groups using the plane-wave method[15] or the exact muffin-tin orbitals (EMTO) method[16] also got similar results, that both α' and α'' phases are metastable phases and the thermodynamic stable phases of cerium are α phase (low pressure) and bct phase (high pressure).

Although the $4f$ electrons in the α phase are delocalized, the strong repulsive interaction among them still modifies its electronic structure significantly. Due to the insufficient treatment of the correlation effects, the bonding strength of the α cerium has been over estimated by the LDA-type calculations, which leads to smaller volume and larger bulk modules compared with the experimental data. In the present paper, we apply the newly developed LDA+Gutzwiller method, which can satisfactorily treat the strong correlation effects in the $4f$ shell, to determine the thermodynamic stable phase of cerium under pressure. We first apply the above method to study the ground-state properties of α cerium under the ambient pressure. Our results show that both the volume and bulk modules are improved dramatically, which manifests the importance of the strong correlation effect for the $4f$ electrons in α cerium. Further we apply the same method to study the intermediate pressure phases of cerium, and the results show that in the intermediate-pressure region the α'' phase is

the thermodynamic stable phase and all other structures are either metastable or unstable, which is quite consistent with the recent experiments.[9, 10]

The rest of the paper is organized as follows: A brief introduction of the LDA+Gutzwiller method are given in Sec. II. In Sec. III we discuss the main results of our LDA+Gutzwiller calculations with the comparison to the recent experimental results and LDA/GGA results. The summary and conclusions are given in the last section.

II. LDA+GUTZWILLER METHOD

Gutzwiller first introduced the Gutzwiller variational approach to study the itinerant ferromagnetism in systems with partially filled d bands described by the Hubbard model.[17] Since then, the Gutzwiller variational approach has been widely applied to various strongly correlated systems.[18–22] Recently, we developed a computational method to incorporate LDA with the Gutzwiller variational approach, named the LDA+Gutzwiller method (simply called LDA+G hereafter),[23–25] by successfully applying to a number of typical correlated materials, the reliability and feasibility of this method have been demonstrated. In the following we present the method briefly; please refer to our previous paper[25] for more details.

Similar to LDA+U and LDA+DMFT methods, in LDA+G the LDA Hamiltonian, which can be extracted from the first-principles calculation, is implemented by a Hubbard-like local Coulomb interaction, which is not adequately treated within LDA. The effect of this local Coulomb interaction can thus be considered within the Gutzwiller variational approach. The Hamiltonian can be usually expressed as

$$H = H_{LDA} + H_{int} - H_{DC}, \quad (1)$$

with

$$H_{int} = \sum_{i,\alpha,\beta(\alpha\neq\beta)} \mathcal{U}_i^{\alpha,\beta} \hat{n}_{i\alpha} \hat{n}_{i\beta}, \quad (2)$$

where H_{LDA} is the LDA part of the Hamiltonian extracted from the standard LDA calculation, H_{int} is the on-site interaction term, where α and β are combined spin-orbit indices of localized basis $\{\phi_{i,\alpha}\}$ on site i , among which the local Hubbard interaction is implemented, $\alpha = 1, \dots, 2N$ (N is the orbital number, e.g., $N = 7$ for f electrons). H_{DC} is the dou-

ble counting term representing the average orbital independent interaction energy already included by LDA. Without the H_{int} term, the ground state can be exactly given by the Kohn-Sham uncorrelated wave function (KSWF) $|\Psi_0\rangle$, which is a single Slater determinant made from the single-particle wave functions. However, with the increment of the interaction strength, the KSWF is no longer a good approximation because it gives too much weighting factor for those energetically unfavorable configurations. In order to give a better description of the ground state, the weighting factor of those unfavorable configurations should be suppressed, which is the main idea of Gutzwiller wave functions (GWFs) $|\Psi_G\rangle$. A GWF is constructed by a many-particle projection operator acting on the uncorrelated KSWF, which reads

$$|\Psi_G\rangle = \hat{P}|\Psi_0\rangle = \prod_i \hat{P}_i|\Psi_0\rangle, \quad (3)$$

with

$$\hat{P}_i = \sum_{\Gamma} \lambda_{i\Gamma} \hat{m}_{i\Gamma}, \quad (4)$$

$$\hat{m}_{i\Gamma} = |i, \Gamma\rangle \langle i, \Gamma|, \quad (5)$$

where $\hat{m}_{i\Gamma}$ is the projector to the specified configuration $|\Gamma\rangle$ on site i . In Eq. (3), the role of projection operator \hat{P} is to adjust the weight of each atomic configuration through variational parameters $\lambda_{i\Gamma}$ ($0 \leq \lambda_{i\Gamma} \leq 1$). The GWF falls back to KSWF if all $\lambda_{i\Gamma} = 1$. On the other hand, if $\lambda_{i\Gamma} = 0$, the configuration $|\Gamma\rangle$ on site i will be totally removed. In this way, both the itinerant behavior of uncorrelated wave functions and the localized behavior of atomic configurations can be described consistently, and the GWF can give a more accurate description of the correlated metallic systems than KSWF.

The total energy of the above system can be expressed as the expectation value of the Hamiltonian equation (1) using GWF, which takes the form

$$E_{Total} = \langle \Psi_G | H | \Psi_G \rangle = \langle \Psi_G | H_{LDA} | \Psi_G \rangle + \langle \Psi_G | H_{int} | \Psi_G \rangle - E_{DC}, \quad (6)$$

In Eq. (6), the interaction energy is given as

$$\langle \Psi_G | H_{int} | \Psi_G \rangle = \sum_{i,\Gamma} E_{i\Gamma} m_{i\Gamma}, \quad (7)$$

where $m_{i\Gamma}$ is the weight of configuration Γ ,

$$m_{i\Gamma} = \langle \Psi_G | \hat{m}_{i\Gamma} | \Psi_G \rangle \quad (8)$$

According to Eq. (3), the LDA energy of Eq. (6) can be written as

$$\langle \Psi_G | H_{LDA} | \Psi_G \rangle = \langle \Psi_0 | \hat{P} H_{LDA} \hat{P} | \Psi_0 \rangle = \langle \Psi_0 | H_{LDA}^G | \Psi_0 \rangle. \quad (9)$$

H_{LDA}^G is called the effective Hamiltonian under Gutzwiller approximation.

The DFT calculations for realistic materials are always done in reciprocal space, so the formulas above should transform to the reciprocal space. We define the Bloch states of localized orbitals $|i\alpha\rangle$

$$|k\alpha\rangle = \frac{1}{N} \sum_i e^{ikR_i} |i\alpha\rangle \quad (10)$$

Then H_{LDA}^G in k space can be written as

$$\begin{aligned} H_{LDA}^G = & \left(\sum_{k\alpha} z_\alpha |k\alpha\rangle \langle k\alpha| + 1 - \sum_{k\alpha} |k\alpha\rangle \langle k\alpha| \right) \\ & H_{LDA} \left(\sum_{k'\beta} z_\beta |k'\beta\rangle \langle k'\beta| + 1 - \sum_{k'\beta} |k'\beta\rangle \langle k'\beta| \right) \\ & + \sum_{kk'\alpha} (1 - z_\alpha^2) |k\alpha\rangle \langle k'\alpha| H_{LDA} |k'\alpha\rangle \langle k\alpha|, \end{aligned} \quad (11)$$

where z_α is the renormalization factor for local orbital α , which depends on those Gutzwiller variational parameters λ_Γ ; for those noninteracting orbitals, the corresponding z factor equals 1.

According to Eqs. (6), (7), (9), and (11), the total energy reads

$$\begin{aligned} E_{Total} = & \langle \Psi_0 | \left(\sum_{k\alpha} z_\alpha |k\alpha\rangle \langle k\alpha| + 1 - \sum_{k\alpha} |k\alpha\rangle \langle k\alpha| \right) \\ & H_{LDA} \left(\sum_{k'\beta} z_\beta |k'\beta\rangle \langle k'\beta| + 1 - \sum_{k'\beta} |k'\beta\rangle \langle k'\beta| \right) | \Psi_0 \rangle \\ & + \sum_\alpha (1 - z_\alpha^2) n_\alpha \varepsilon_{LDA}^\alpha + \sum_\Gamma E_\Gamma m_\Gamma - E_{DC}, \end{aligned} \quad (12)$$

where $\varepsilon_{LDA}^\alpha = \sum_k \langle k\alpha | H_{LDA} | k\alpha \rangle$ and $n_\alpha = \sum_k \langle \Psi_0 | k\alpha \rangle \langle k\alpha | \Psi_0 \rangle$.

The total energy expressed in Eq. (12) depends on both the uncorrelated “starting” wave function $|\Psi_0\rangle$ and those Gutzwiller variational parameters λ_Γ , which can both be determined by minimizing the total energy. After we obtain the ground-state wave function, we can calculate most of the ground-state properties based on it; please refer to our paper[25] for more details.

III. RESULTS AND DISCUSSIONS

Like LDA+U and LDA+DMFT methods, in LDA+G the Hubbard-like local Coulomb interaction U will be chosen as the only empirical parameter. First we calculate the equilibrium volume for α -Ce (fcc) to check the validity of the different U value as shown in Fig. 1. The volume of Ce under ambient pressure is between 28.0 and 29.0 \AA^3 reported experimentally,[5, 8] so the equilibrium volume for $U = 4.0$ eV (28.49 \AA^3) is in good agreement with experiments, while the equilibrium volume for $U = 3.5$ eV (around 27.5 \AA^3) and $U = 4.5$ eV (around 29.5 \AA^3) are smaller and larger than experiments, respectively. We also calculate the bulk modulus for α -Ce under ambient pressure as shown in Table I together with the results from the all-electron FPLMTO calculations,[26] pseudopotential plane-wave calculations,[15] and experiments.[5, 8] We can see from the table that the LDA calculation usually over-estimates the bonding strength among cerium atoms, which makes the equilibrium volume obtained by LDA to be about 20% smaller and bulk modulus to be much larger than experiments. After treating the correlation effect more carefully by the Gutzwiller variational method, our results are in good agreement with experiments. Thus we set $U = 4.0$ eV for all the calculations for cerium with different volume, which is consistent with other LDA+U and DMFT calculations, and spin-orbital coupling effect is always fully included.

Early experiments have reported two intermediate-pressure phases of cerium, α' phase and α'' phase, together with the low-pressure α phase and high-pressure bct phase. The thermodynamic stability of these four phases under pressure is the main interest of the present work. Neglecting the tiny distortion in the α'' phase, all these three phases including α , α'' , and the high-pressure bct phase can be treated within the same bct structure but with the different ratio of the lattice constants c/a , [8, 9, 13] which is illustrated in Fig. 2.

The c/a ratio is exactly $\sqrt{2}$ for α phase with the fcc structure and is found to be around 1.65 for the high-pressure bct phase. The c/a ratio of the α'' phase is reported experimentally to be around $1.5 \leq c/a \leq 1.56$. [5, 8] Therefore in the present paper, we first apply the LDA+G method to minimize the enthalpy of the cerium with bct structure with respect to the c/a ratio as the function of pressure, which mimics the competition among the α , α'' , and high-pressure bct phases under pressure, and after that we will compare the enthalpy of these phases and the α' phase. Our main results have been plotted in Fig. 3 with the comparison to LDA and GGA. The results obtained by all three methods agree quite well for pressure less than 9.0 GPa indicating that the α phase (fcc) with $c/a = \sqrt{2}$ is the thermodynamic stable structure. For pressure between 9.0 and 25.0 GPa, the results obtained by LDA, GGA, and LDA+G are quite different. First of all, all three methods predict that all phases appear as the locally stable phases in this intermediate pressure region, while LDA results indicate that the α'' phase is the thermodynamic stable phase in a very small region around 17.0 GPa. Although GGA gives a reasonably wide region from 23.0 to 27.0 GPa, within which the α'' phase is globally stable, this pressure region is much higher than the experimental results, which is from 6.9 to 12.0 GPa. [8] LDA+G predicts that the α'' phase is the thermodynamic stable phase in the pressure region of 13.0–17.0 GPa, which is much closer to the experimental data. [8] For pressure larger than 25.0 GPa, all three methods again reach the same conclusion that the high-pressure bct phase is thermodynamic stable, whereas the other two are either metastable or unstable.

The optimized c/a ratio as the function of pressure for Ce obtained from our LDA, GGA, and LDA+G calculations are plotted in Fig. 4 together with the experimental results. [8] We can find clearly that the LDA+G calculation obtains the globally stable region of α'' -Ce to be from 13.0 to 17.0 GPa, which is much closer to the experimental data, [8] while LDA only gets a very narrow region for α'' -Ce stable, and GGA gets the α'' phase stable in a pressure region that is much higher than experimental data, as shown in Fig. 4.

The next issue to be addressed is the relative enthalpy of the α' phase compared with the other three phases discussed in the previous paragraph. The α' phase has a orthorhombic α -U structure, which can be viewed as distorted fcc with some of the face-centered atoms being shifted from their original positions, as described by the parameter $2y$. [11] The $2y$ value obtained experimentally by McMahon and Nelmes [9] is 0.2028 Å. If $2y = 0.5$ Å and $a = b = c$, the standard fcc structure can be restored. Therefore we can calculate the energy

of α -Ce (fcc) and α' -Ce within the same α -U structure. We use $a/b = 0.5115, c/b = 0.8756$ as obtained from the experiment,[9] and optimize the $2y$ value for any given volume. We find that $2y = 0.21$ gives the minimum energy for volume being 22.5 \AA^3 , which is in good agreement with experiment.[9] We calculated the enthalpy of α -Ce (fcc) and α' -Ce within the same α -U structure frame for a pressure region: $9.0 \text{ GPa} \leq P \leq 21.0 \text{ GPa}$. The enthalpy difference between them ($H_{\alpha'} - H_{\alpha}$) is plotted in Fig. 5 together with the enthalpy difference of $H_{\alpha''} - H_{\alpha}$ and $H_{bct} - H_{\alpha}$ obtained previously. Our results confirm that the α' phase is always higher in enthalpy in the entire pressure region considered in the present paper. We thus rule out the α' structure as a thermodynamic stable intermediate pressure phase of cerium. This conclusion is in good agreement with the FPLMTO calculations.[14] From Fig. 5 we can also see that the α'' structure is the thermodynamic stable phase among the above-mentioned four possible phases within the pressure region 13.0–17.0 GPa. Therefore, based on the LDA+G calculation, we conclude that the α'' phase is the thermodynamic stable phase for cerium in the intermediate pressure region. This conclusion is quite consistent with the most recent experiments.[9, 10]

Based on the calculations in the previous paragraph, we obtain the multiphase equations of state (EOSs) for cerium metal, as shown in Fig. 6 together with the experimental data. The agreement between LDA+G results and the experimental data[8] is very good, while the GGA curve is slightly away especially in the low-pressure region and the LDA result is further away from the experimental data.

In Fig. 7, we plot the renormalization factor of the $4f$ bands in the α , α'' , and high-pressure bct phases as the function of volume. We can find that the renormalization factor of the $4f$ bands decreases monotonically with the increment of the volume for all the three phases, which can be easily explained by the fact that increasing volume reduces the hopping integral between the neighboring f orbitals, which enhances the correlation effect among $4f$ electrons and thus reduces the corresponding renormalization factor. From the present LDA+G calculation, we find that the main consequence of the correlation effect in the total energy is to reduce the kinetic energy. Since the fcc structure is close packed, compared with the α'' phase, the α phase has relatively higher kinetic energy gain, which is overcounted by LDA. Because of that, the reduction of kinetic energy gain captured by LDA+G is also more pronounced in the α phase, which raises the total energy of the α phase relative to the α'' phase and makes it thermal dynamically unstable in the intermediate pressure

region. We would like to emphasize that the renormalization factor obtained in Gutzwiller approximation is defined by the reduction of the kinetic energy, which is in general higher than that obtained by dynamical mean-field theory through the quasiparticle spectral weight of the Green's function. Please refer to our previous paper for the detailed discussion on this point.[24]

IV. CONCLUSIONS

In summary, using the newly developed LDA+G technique, we have carried out systematic numerical study on the phase diagram of cerium metal under pressure. We found that the correlation effect among f electrons in cerium plays a crucial role to determine the thermodynamic stable phase of cerium in the intermediate pressure region. The LDA calculation overestimates the chemical bonding contributed by the $4f$ electrons, which leads to smaller equilibrium volume and larger bulk modulus compared to the experimental data. With the increment of pressure, the overlap between $4f$ orbitals becomes more and more pronounced, which reduces the correction to the total energy caused by the correlation effect. Therefore the correct description of the correlation effect, which evolves with the pressure, becomes one of the key issues to obtain the correct phase diagram in the intermediate pressure region. Our numerical results obtained by the LDA+G method conclude that the α'' phase is the thermodynamic stable phase in the intermediate-pressure region, which is quite consistent with the recent experiments.

ACKNOWLEDGMENTS: The authors thank L. Wang, J. N. Zhuang, G. Xu, and Q. M. Liu for their helpful discussions. We acknowledge the support from the 973 Program of China (Grant No. 2007CB925000), from the NSF of China (Grants No. NSFC 10876042 and No. NSFC 10874158), and that from the Development Foundation of CAEP (Grant No. 2008A0101001).

-
- [1] K. A. Gshneidner, Jr., R. O. Elliott, and R. R. McDonald, *J. Phys. Chem. Solids* **23**, 555 (1962).
- [2] K. Haule, V. Oudovenko, S. Y. Savrasov, G. Kotliar, *Phys. Rev. Lett.* **94**,036401 (2005).

- [3] K. Held, A. K. McMahan, and R. T. Scalettar, Phys. Rev. Lett. **87**, 276404 (2001).
- [4] B. Amadon, S. Biermann, A. Georges, F. Aryasetiawan, Phys. Rev. Lett. **96**, 066402 (2006).
- [5] F. H. Ellinger and W. H. Zachariasen, Phys. Rev. Lett. **32**, 773 (1974). W. H. Zachariasen and F. H. Ellinger, Acta Crystallogr. Sec. A **33**, 155 (1977).
- [6] Guoliang Gu, Yogesh K. Vohra, and Keith E. Brister, Phys. Rev. B **52**, 9107 (1995).
- [7] Y. C. Zhao and W. B. Holzapfel, J. Alloys Compd. **246**, 216 (1997).
- [8] J. Staun Olsen, L. Gerward, U. Benedict, and J. P. Itié, Physica B **133**, 129 (1985)
- [9] M. I. McMahon and R. J. Nelmes, Phys. Rev. Lett. **78**, 3884 (1997).
- [10] V. P. Dmitriev, A. Yu. Kuznetsov, O. Bandilet, P. Bouvier, L. Dubrovinsky, D. Machon, and H.-P. Weber, Phys. Rev. B **70**, 014104 (2004).
- [11] Hans L. Skriver, Phys. Rev. B **31**, 1909 (1985)
- [12] J. M. Wills, O. Eriksson and A. M. Boring, Phys. Rev. Lett. **67**, 2215 (1991). O. Eriksson, J. M. Wills, and A. M. Boring, Phys. Rev. B **46**, 12981 (1992).
- [13] P. Söderlind, O. Eriksson, B. Johansson, and J. M. Wills, Phys. Rev. B **52**, 13169 (1995). P. Söderlind, Adv. Phys. **47**, 959 (1998).
- [14] P. Ravindran, L. Nordström, R. Ahuja, J. M. Wills, B. Johansson, O. Eriksson, Phys. Rev. B **57**, 2091 (1998).
- [15] Nicolas Richard and Stéphane Bernard, J. Alloys Compd. **323**, 628 (2001).
- [16] A. Landa, P. Söderlind, A. Ruban, L. Vitos and L. Pourovskii, Phys. Rev. B **70**, 224210 (2004).
- [17] M. C. Gutzwiller, Phys. Rev. Lett. **10**, 159 (1963); Phys. Rev. **134**, 923 (1964); **137**, 1726 (1965).
- [18] W. F. Brinkman and T. M. Rice, Phys. Rev. B **2**, 4302 (1970).
- [19] D. Vollhardt, Rev. Mod. Phys. **56**, 99 (1984). F. Gebhard and D. Vollhardt, Phys. Rev. Lett. **59**, 1472 (1987); Phys. Rev. B **38**, 6911 (1988). D. Vollhardt, P. G. J. Van Dongen, F. Gebhard, and W. Metzner, Mod. Phys. Lett. B **4**, 499 (1990).
- [20] F. C. Zhang, C. Gros, T. M. Rice, and H. Shiba, Supercond. Sci. Technol. **1**, 36 (1988).
- [21] W. Metzner and D. Vollhardt, Phys. Rev. Lett. **59**, 121 (1987); Rev. B **37**, 7382 (1988); Phys. Rev. Lett. **62**, 324 (1989); W. Metzner, Z. Phys. B: Condens. Matter **77**, 253 (1989).
- [22] J. Bünemann, F. Gebhard, and W. Weber, J. Phys.: Condens. Matter **9**, 7343 (1997); J. Bünemann and W. Weber, Phys. Rev. B **55**, 4011 (1997); J. Bünemann, W. Weber, and F. Gebhard, *ibid.* **57**, 6896 (1998); J. Bünemann, F. Gebhard, and W. Weber, Found. Phys. **30**,

- 2011 (2000); C. Attaccalite and M. Fabrizio, Phys. Rev. B **68**, 155117 (2003).
- [23] G. T. Wang, X. Dai, and Z. Fang, Phys. Rev. Lett. **101**, 066403 (2008).
- [24] XiaoYu Deng, Xi Dai and Zhong Fang, Eur. Phys. Lett. **83**, 37008 (2008).
- [25] XiaoYu Deng, Lei Wang, Xi Dai, and Zhong Fang, Phys. Rev. B **79**, 075114 (2009).
- [26] P. Söderlind, O. Eriksson, J. Trygg, B. Johansson, J.M. Wills, Phys. Rev. B **51**, 4618 (1995).

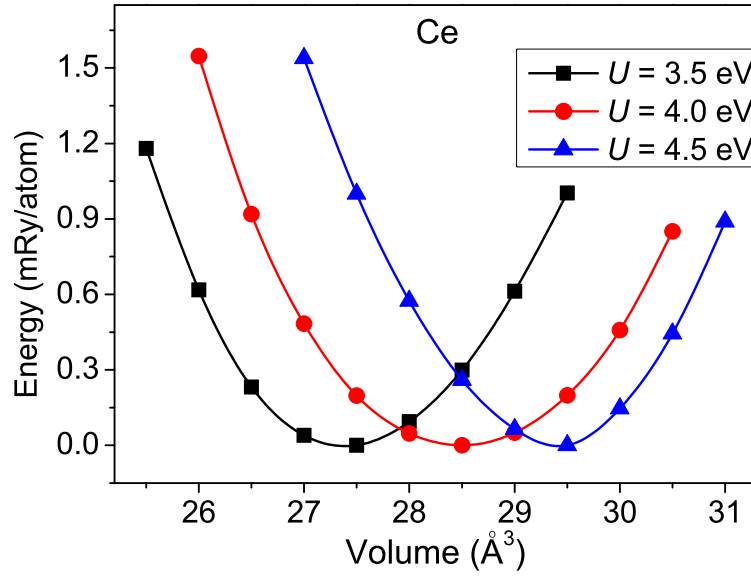


FIG. 1: (Color online) Calculated energy curves of α -Ce (fcc) as a function of atomic volume for different values of U by LDA+G method.

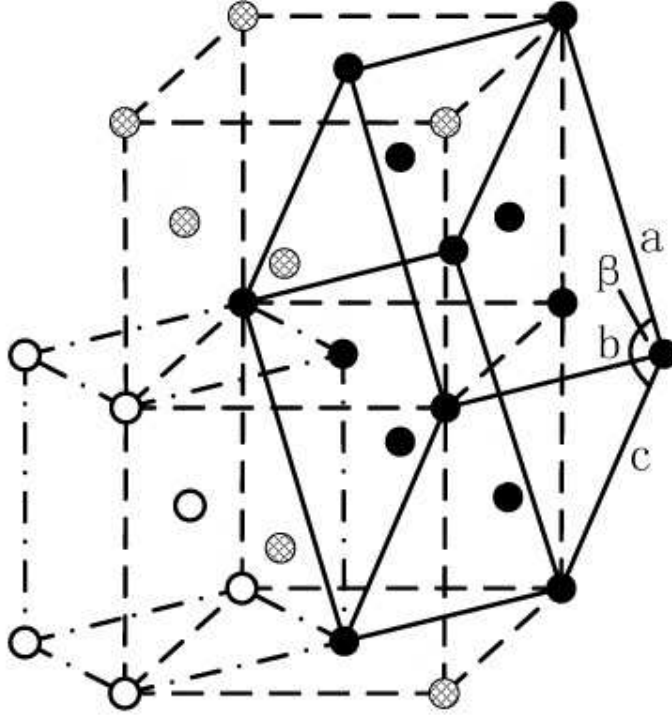


FIG. 2: The relationship between the α phase (face-centered cubic, dashed lines with hatched circles—main cell), bct phase (body-centered tetragonal, dash-dot line subcell with unfilled circles), and the α'' phase (C-face-centered monoclinic, solid line subcell with black circles).

TABLE I: Theoretical and experimental values of the equilibrium volume V and bulk modulus B for α -Ce from our LDA+G calculations, some LDA/GGA calculations (Refs. [15] and [26]), and experimental data (Refs. [5] and [8]).

	V (\AA^3)	B (GPa)
LDA	23.3[15], 22.74[26]	58.7[15], 60.5[26]
GGA	26.3[15], 26.05[26]	43.0[15], 48.7[26]
Experiment[5, 8]	28-29	20-35
Present (LDA+G)	28.49	27.6

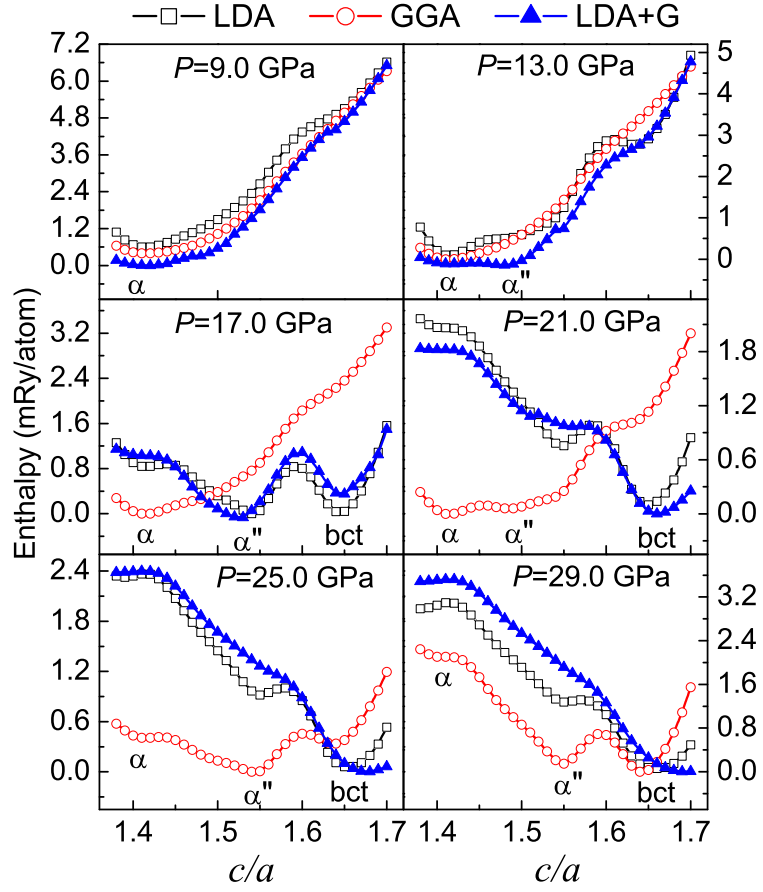


FIG. 3: (Color online) Calculated enthalpy of body-centered-tetragonal Ce as a function of c/a axial ratio by LDA, GGA, and LDA+G methods, respectively.

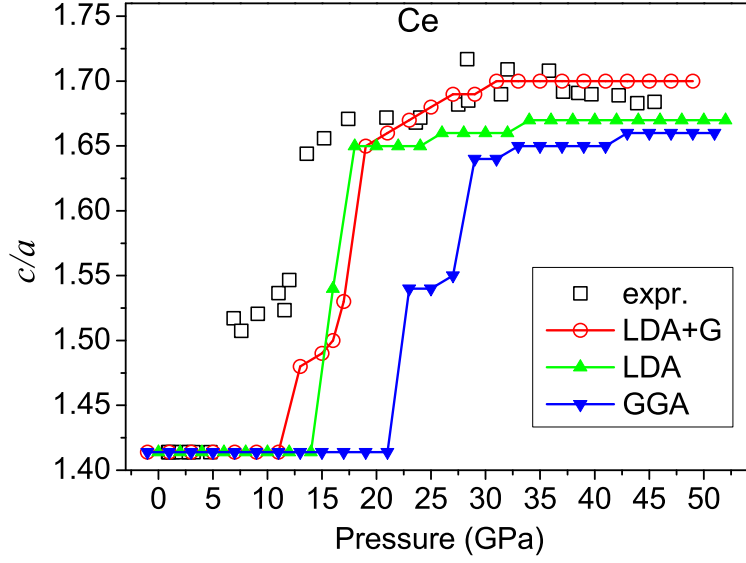


FIG. 4: (Color online) The c/a axial ratio for the body-centered tetragonal structure as a function of pressure for Ce. Experimental data (Ref. [8]) are marked with black open squares, while LDA+G results are given by a red solid line and open circles. LDA results are given by a green solid line and filled uptriangles, and the results of GGA are shown by a blue solid line and filled downtriangles.

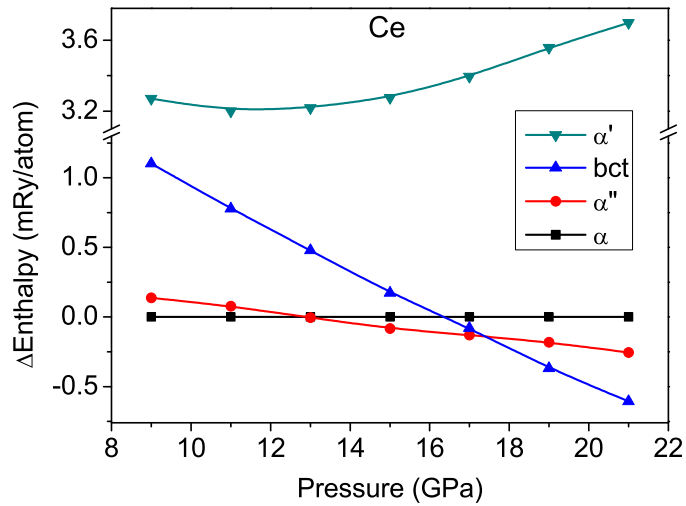


FIG. 5: (Color online) The enthalpy curves for the intermediate-pressure phases of Ce relative to the α phase (fcc) as obtained from LDA+G calculations.

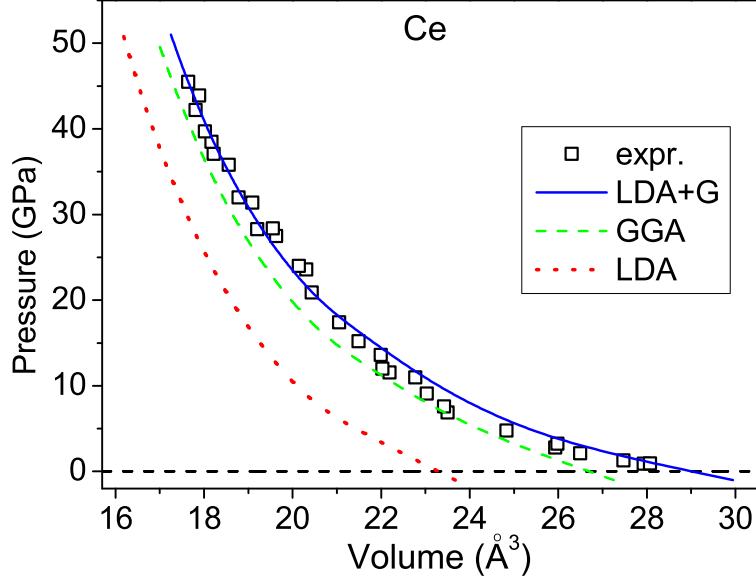


FIG. 6: (Color online) Equation of state for Ce. Experimental results (Ref. [8]) are marked with open squares and theory is given by lines.

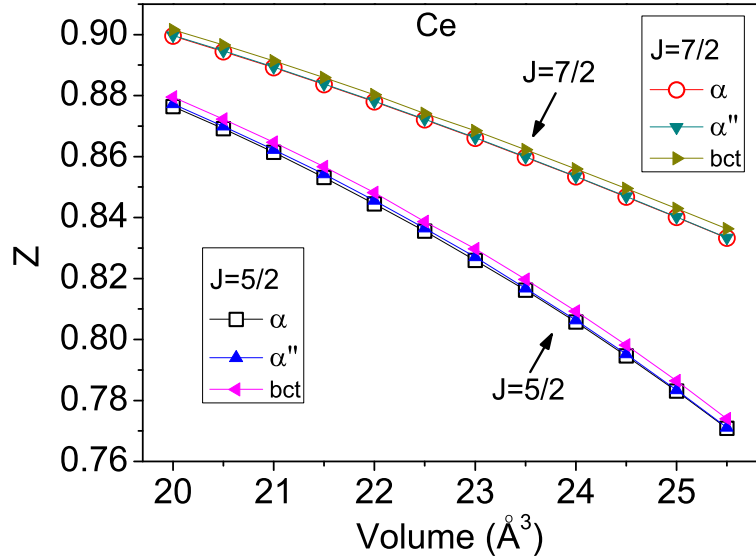


FIG. 7: (Color online) The average renormalization factor as a function of volume for angular momentum $J = 5/2$ and $J = 7/2$ f electrons of Ce.